Pressure induced phase transitions and equation of state of adamantane

2001 J. Phys.: Condens. Matter 13 1961

(http://iopscience.iop.org/0953-8984/13/9/318)

INSTITUTE OF PHYSICS PUBLISHING JOURNAL OF PHYSICS: CONDENSED MATTER

J. Phys.: Condens. Matter **13** (2001) 1961–1972 www.iop.org/Journals/cm PII: S0953-8984(01)18706-0

Pressure induced phase transitions and equation of state of adamantane

V Vijayakumar, Alka B Garg, B K Godwal and S K Sikka

High Pressure Physics Division, Solid State and Spectroscopy Group, Purnima Laboratories, BARC, Mumbai 400085, India

E-mail: bkgodwal@magnum.barc.ernet.in

Received 29 November 2000, in final form 11 January 2001

Abstract

Results of angle dispersive x-ray powder diffraction measurements under pressure up to 25 GPa on adamantane carried out at the synchrotron source SPRING-8 are reported. The disorder–order transition at 0.5 GPa in adamantane known earlier is reproduced with detailed structural information. For this ordered tetragonal ($P\bar{4}2_1c$, $z = 2$) phase, the shortest intermolecular hydrogen separation (H . . . H) reduces from 2.37 Å at 0.7 GPa to 1.87 Å at 12.5 GPa and the relative angle of rotation (ϕ) of the two molecules within the cell about the c-axis increases from 8.5° to 10.5°. This is consistent with values determined from energy minimization in this pressure region. The anomaly in the pressure variation of c/a, and the failure of the constrained Rietveld refinement, occurring close to 9 GPa, are interpreted as due to distortion of the adamantane molecule when H . . . H distance decreases below the critical value of 1.9 Å. Above 16 GPa there is a subtle change in the diffraction pattern that indicates a transition to a closely related phase. Beyond 22 GPa, a monoclinic phase with one molecule per cell could only index the patterns. The ambient cubic phase is recovered on unloading indicating the absence of decomposition or polymerization. The results of high pressure x-ray diffraction experiments confirm the changes in the Raman spectra observed in the earlier measurements.

1. Introduction

The x-ray diffraction measurements at high pressure on organic molecular solids are very few. Various factors like low symmetry and large volume unit cells of the crystals, weak x-ray scattering by the constituent atoms, small volume of the polycrystalline sample that a diamond anvil cell can hold etc are responsible for this. However, availability of flat area detectors (X-CCD and imaging plate) that allow fast data collection, use of state of the art processing techniques that improve signal to noise ratio and third generation synchrotron sources have changed the scenario substantially. Now it is possible to extract meaningful structural information on molecular solids through constrained Rietveld refinement of high pressure x-ray powder diffraction data.

0953-8984/01/091961+12$30.00

The adamantane ($C_{10}H_{16}$) molecule is highly symmetrical with the carbon skeleton in it made up of four interlocking six membered C rings having zero strain with all the C–C–C bond angles at 109.45°. At ambient conditions it crystallizes in a cubic phase (space group $Fm3m$, $Z = 4$) with molecules orientationally disordered and is a prototypical example of a plastic molecular crystal. It is an organic crystal possessing high symmetry and is an example of the preservation of the molecular point group symmetry (T_d) in the solid. The molecules in the ambient phase have an ellipsoidal shape with the major and minor radii (half the distance between two methylene carbons and perpendicular to this direction) of 1.719 Å and 1.554 Å respectively. It transforms to an ordered tetragonal phase ($P\bar{4}2_1c$) with two molecules per cell either by cooling below 208 K or by pressurizing above 0.5 GPa (Ito 1973), the volume decrease at both transitions is about 3.5%. Amoureux and Foulon (1987) have given the structural details by carrying out low temperature single crystal x-ray diffraction work. The 'radii' of the molecule in this phase are 1.765 Å and 1.530 Å indicating a slight distortion of the molecule compared to the ambient cubic case. The molecules are ordered and packed like hard ellipsoids with more squashing in the c-direction having a packing coefficient of 0.757. The H . . . H separation between the neighbouring molecules is 2.37 Å, twice the van der Waals radius of hydrogen atom. On the other hand the C–C bond lengths (1.53 Å) are close to that in diamond implying that it will only be moderately compressible. With the application of pressure, the weak non-bonded H . . . H separations will decrease and ultimately reach the empirical limiting value of 1.9 Å (Steiner and Saenger 1991, Sikka and Sharma 1992) below which the further reduction is forbidden due to steric hinderance (Sikka and Sharma 1992, Sikka 1997a, b). Even before this critical value is reached, the reduced H . . . H separations will make a repulsive contribution to the total energy, inducing phase transitions accompanied by changes in molecular arrangements or distortions to relieve the repulsive strains. In fact, the low temperature phase transition is brought about by this mechanism. This is clear from the fact that H . . . H distances as obtained from single crystal data increase from 2.23 Å in the cubic phase to a value of 2.37 Å in the tetragonal phase on transition. Altering the relative tilting of the two adamantane molecules in the $P\bar{4}2_1c$ structure is the means by which the crystal relieves the H . . . H repulsion. The chemical stability further limits the H . . . H distance because, if the H . . . H distance approaches the H-H covalent bond length, it will result in decomposition of the molecule due to the formation of free hydrogen molecule. The hydrogen bonded HBr (Katoh *et al* 1999) decomposes via this route under pressure and number of materials amorphize due to steric constraint (Sikka and Sharma 1992). In addition, because of packing requirements under pressure, there is a possibility of molecular deformation (further squashing) especially after the H . . . H critical distance is reached. Thus under pressure adamantane may undergo deformation of the molecule, structural change, amorphization, hydrogen disorder, polymerization or decomposition.

While there is a large number of experimental and theoretical investigations on the high pressure structural, electronic and vibrational behaviour of fullerenes (Shirl *et al* 1971, Snoke *et al* 1992, Chandrabhas *et al* 1994), simpler carbon based caged molecular solids like adamantane and hexamethylentetramine (Rekha Rao *et al* 1999) are relatively unexplored. It may be noted that the adamantane is the parent compound of a series of molecular solids that have cage structured molecules obtained by replacing hydrogen atoms of adamantane with other ions or groups. Investigations on such systems starting with adamantane is of utility in understanding various molecular interactions and their role in structural transitions under pressure in molecular solids. The previous x-ray work on adamantane (Ito 1973) is limited to 0.8 GPa. Recent Raman measurements on adamantane (Rekha Rao *et al* 2000) up to 26 GPa revealed a number of reversible changes in the internal modes. In addition to the structural change at 0.5 GPa (Ito 1973), the pressure dependence of internal mode frequencies suggested

two subtle reversible transitions around 2.8 and 8.5 GPa. Evolution of Raman spectra at higher pressure showed evidence for two more structural transitions around 16 and 24 GPa. In order to identify the structural origin of these spectral changes we have carried out angle dispersive x-ray diffraction (ADXRD) measurements on adamantane under pressure. Here, we report the details of the structural evolution of adamantane under pressure.

2. Experiment

ADXRD measurements at high pressures were carried out at the BL10 XU beam line of the third generation synchrotron source SPRING-8 in Japan. The Si double monochromator was used to obtain the monochromatized ($\lambda = 0.7$ Å) x-ray beam which was collimated to 80×80 μm^2. The Mao–Bell type diamond anvil cell (DAC) (Vijayakumar and Meenakshi 2000) had a rectangular horizontal opening to cover an angle up to 45° half cone. X-rays diffracted from the sample were detected using a Rigaku image plate area detector aligned normal to the beam. Adamantane along with a ruby chip was loaded in a 100 μm diameter hole of an 80 μm thick hardened stainless steel gasket in the DAC. The pressure was measured by the ruby fluorescence technique. No pressure medium was employed because adamantane is a soft solid and serves as a good pressure medium. It may be noted that a pressure medium if employed may induce/interfere with the possibility of decomposition, polymerization etc. The ruby lines were found to be sharp and well separated to the highest pressure. Due to poor x-ray scattering power of the atoms in $C_{10}H_{16}$, the exposure time for each pressure was about three hours. The collected patterns were processed by radial integration, corrected for detector tilt and appropriate Lorenz polarization factor (flat area detector normal to the beam in the transmission geometry and plane polarized x-rays (Gualtieri *et al* 1996)). The sample to detector distance was obtained from the ambient XRD patterns of KI (loaded in the cell) from two image plate to sample distances with a separation 10.000 cm. The one dimensional diffraction patterns so obtained were used for obtaining the d-values and for carrying out the Rietveld refinement. In spite of the fact that adamantane is a poor x-ray scatterer, we could obtain good diffraction patterns because of the high x-ray beam intensity and due to improved data processing by radial integration. Sixteen (at low pressure) to ten (at the highest pressure) clear Bragg peaks were available for obtaining d-values by peak fitting, which yielded lattice parameters with high precision.

3. Results and discussion

The variation of the diffraction patterns as a function of pressure is shown in figure 1. Above 10 GPa, because of a phase change in the gasket material and slight collapse of the gasket hole, a change in the gasket line position and intensity is seen in figure 1(c). It may be noted that the scattering intensity from the metallic gasket will be exceedingly intense compared to that of the sample and thus a small intensity increase of gasket lines does not imply that x-rays are not hitting the sample. Also the telescopic viewing and centring facility that is available with the beam line ensured that the x-ray beam was passing through the centre of the gasket hole. The pressure variation of the d-values of the prominent lines determined from the processed data do not show any discontinuities (figure 2). This behaviour is analogous to the almost linear pressure variation of various Raman modes up to 16 GPa (Rekha Rao *et al* 2000). It is possible to index the patterns on a tetragonal cell up to the pressure of 18.9 GPa. The relative intensity of various Bragg peaks and their width changed with increasing pressure. Above 8 GPa, even though the ruby lines are sharp, the (112), (201), (002) and (202) lines broadened. Also the

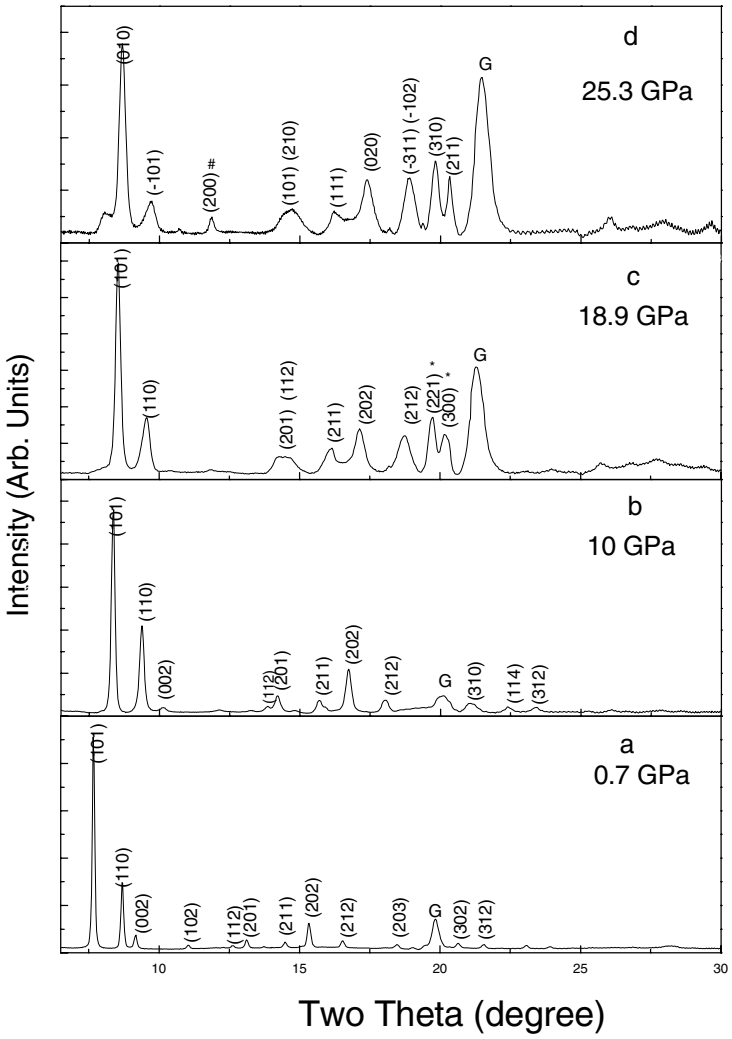

Figure 1. Diffraction patterns of adamantane as a function of pressure. G indicates the gasket line.

(002) and (210) lines merged with the background and the (112) and (201) lines merged with each other above 12 GPa. Figure 3 shows the variation of full width at half maximum (FWHM) of (112) and (201) lines with pressure and indicates a clear fast change in FWHM starting at 8 GPa. This is perhaps due to the increase in the shear strength of adamantame leading to the development of pressure gradient. It may be noted that we did not use ethanol–methanol pressure transmitter, that is known to freeze in this pressure region. However, the ruby lines are sharp in this pressure region and remain to be so to the highest pressure. Thus considering the fact that small ruby pieces may give sharp ruby lines even when there is a pressure gradient, the line broadening and intensity change that is observed is an intrinsic material behaviour. As will be discussed in later sections, close to this pressure the H . . . H separations tend to saturate. At about 16 GPa, considerable change in the intensity of the lines and overall increase in the background was noted along with the appearance of two new diffraction lines (see table 1), which persisted up to the highest pressure. The new lines (221), (300) are not allowed in

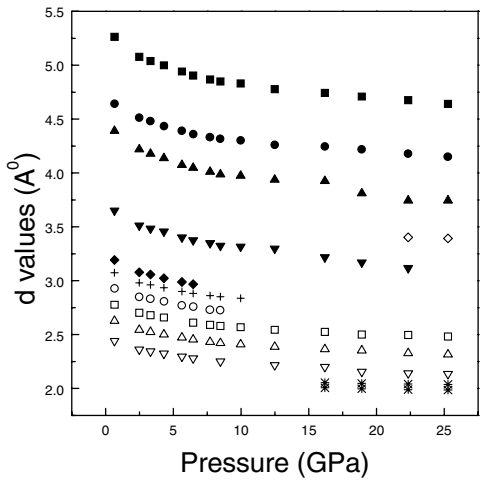

Figure 2. Pressure variation of various d-values.

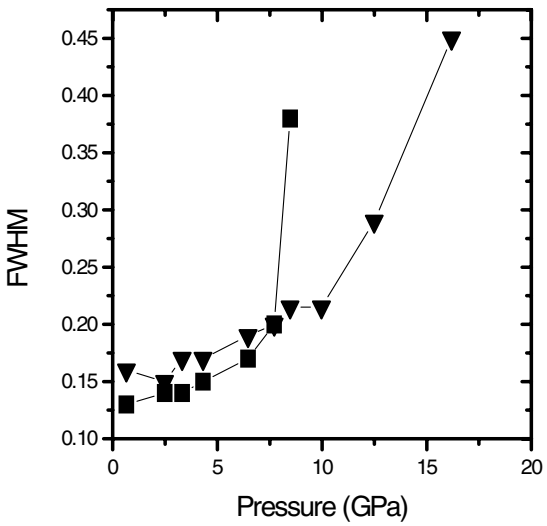

Figure 3. Variation of FWHM of (112 ■) and (201 ▼) lines with pressure.

the SG $P\bar{4}2_1c$, however the pattern continues to be indexable in the same tetragonal cell until 18.9 GPa. Beyond 18.9 GPa, another additional line with d-value of 3.402 Å appeared (table 1). Now a cell of lower symmetry than tetragonal indexes the pattern. It may be noted that even if this weak line is ignored, an indexing on a tetragonal cell is not possible. A monoclinic cell with one molecule per cell can index the pattern well as shown in table 1. Because of the requirement that the cell can have only an integral number of molecules per cell, the high pressure patterns can unambiguously identify the cell as monoclinic. The monoclinic and tetragonal patterns have close resemblance and the approximate dimensional relation between the cells is $a_t = 2^{1/2}\, b_m$, $b_t = 2^{1/2}\, c_m$, $c_t = a_m$. On releasing the pressure from 26 GPa, the ambient pressure cubic phase was recovered, indicating the absence of any polymerization or decomposition of the material.

Table 1. Indexing of the patterns on tetragonal ($a = 6.0114$ Å, $c = 7.7216$ Å) and monoclinic cell ($a = 7.378$ Å, $b = 4.669$ Å, $c = 4.271$ Å, $\beta = 112.6^\circ$) indexing at 22.3 GPa. The indices are given within brackets. The new lines that appeared at 16 GPa (*) and 22 GPa (#) when there was a phase change/space group change are marked. The approximate dimensional relation between the monoclinic and tetragonal cells is $a_t = 2^{1/2}\, b_m$, $c_t = a_m$.

$P = 16.2$ GPa		$P = 22.3$ GPa	
$d_{observed}$	$d_{calculated}$	$d_{observed}$	$d_{calculated}$
Tetragonal		Monoclinic	
4.743	4.743 (101)	4.675	4.669 (010)
4.246	4.250 (110)	4.178	4.179 (−101)
		3.402#	3.406 (200)
2.525	2.538 (211)	2.496	2.498 (111)
2.369	2.371 (202)	2.327	2.334 (020)
2.158	2.125 (220)	2.141	2.140 (−311)
2.053*	2.049 (221)	2.041	2.042 (310)
2.006*	2.003 (300)	1.988	1.986 (211)
1.579	1.581 (303)	1.566	1.556 (030)

On computing the diffraction patterns in the tetragonal phase with and without hydrogen atoms we found that it is the intensity of the (112), (201) and (202) lines that is affected by removal of hydrogen atoms. It is interesting to note that in Raman spectra near 16 GPa, the widths of various C–H modes increases and the intensity decreases (Rekha Rao *et al* 2000). To develop the structural model for this a high pressure neutron diffraction study will be required. A constrained Rietveld refinement of the powder x-ray diffraction patterns was carried out for extracting more structural information. The software DEBVIN (Immirzi 1980) with the provision for constraining the molecular shape (C–C bond length, C–C–C, C–C–H and H–C–H bond angle and C–C–C–H torsion angle) was employed. C–C distances and C–C–C angles and the trial atom positions for the pattern at 0.7 GPa were generated from the carbon and hydrogen position parameters of the ambient pressure low temperature x-ray single crystal data (Amoureux and Foulon 1987). An analysis of the low temperature ambient pressure structure (Pilati 1998) facilitated generation of the structural model and its analysis. It revealed that even the single crystal x-ray data (Amoureux and Foulon 1987) did not locate hydrogen atoms correctly. The hydrogen position was thus adjusted by setting all bond angles (H–C–H, C–C–H) and C–H bond lengths to 109.45° and 1.08 Å (Hamilton 1968) respectively. We refined the lattice parameters, background, line shape and carbon positions with constraints on all intramolecular C–C distances and C–C–C angles (1.53 Å and 109.45° respectively). Hydrogen positions were not refined; instead, employing the provisions of DEBVIN they were attached to the carbon atoms at positions satisfying the above H–C–H, C–C–H angular and C–H bond constraints. For higher pressure runs, the previous lower pressure atom positions were employed as starting values and good fits (R factor of the order of 7%) were obtained up to 9 GPa. Above this pressure, the fit deteriorated and the R factor increased to 22% at 12.5 GPa indicating that the assumption of a constrained molecule is not valid here. Because of this the refinement was terminated at this pressure. Figure 4 shows the Rietveld refined spectra along with the measured ones at 0.7, 10.0 and 12.5 GPa. Table 2 lists the refined atom positions at 0.7 and 10.0 GPa and figure 5 illustrates the features of the molecular arrangement when viewed along the c-axis. The tetragonal phase at 0.7 GPa (see table 2 for atom positions) is almost identical to that of the ambient pressure low temperature phase with both having nearly the same c/a, cage diameters (1.759 Å and 1.522 Å) and intermolecular hydrogen distances. In this phase with two molecules per cell, the molecules are centred at (000) and (1/2,1/2,1/2)

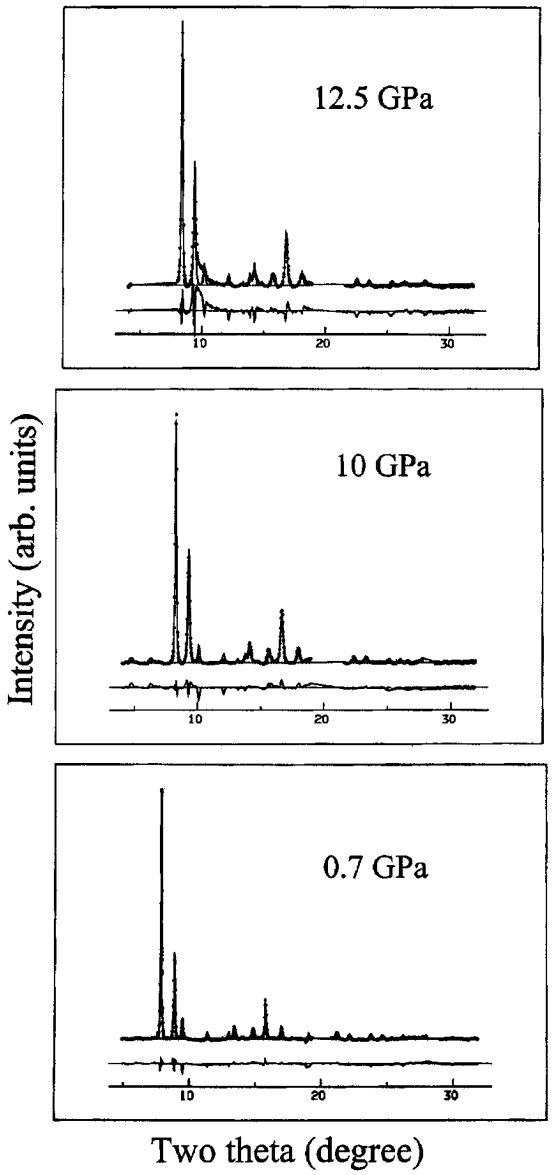

Figure 4. The results of Rietveld refinement at 0.7, 10.0 and 12.5 GPa.

but rotated about the c-axis by 8.5° (ϕ). Thus we confirm that the high pressure and low temperature phases are identical.

From the analysis of the atom positions obtained from Rietveld refinements, it was observed that the intermolecular hydrogen separation reduces rapidly with pressure from 2.37 Å at 0.7 GPa and tends to saturate at 1.87 Å as shown in figure 6. The relative intermolecular angle of rotation (ϕ) of the two molecules (figure 5) within the cell about the c-axis increases from 8.5° at 0.7 GPa to 10.5° at 12.5 GPa. In order to establish that the constrained Rietveld refined structural parameters are realistic, the intermolecular non-bonded energy of the central molecule of a cluster in the crystal was calculated using two body

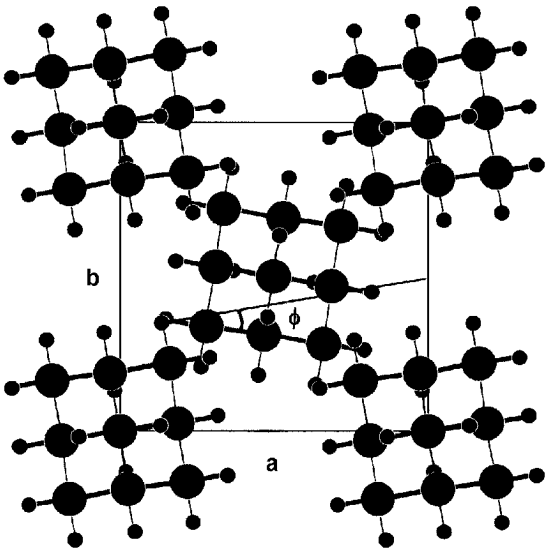

Figure 5. Tetragonal structure of adamantane at 0.7 GPa viewed along the c-axis. Two adjacent molecules are rotated about the c-axis in opposite directions. The relative angle of rotation (ϕ) is 8.5° at 0.7 GPa, which increases to 10.2° at 10.0 GPa. Smaller spheres are hydrogen atoms.

Table 2. The fractional atom position parameters of adamantane at 0.7 GPa pressure ($a = 6.551$ Å, $c = 8.796$ Å) and at 10 GPa ($a = 6.07$ Å, $c = 7.914$ Å).

	$P = 0.7$ GPa			$P = 10$ GPa		
Atom	X	Y	Z	X	Y	Z
C(1)	0	0	0.200	0	0	0.223(1)
C(2)	−0.028	0.188	0.1	−0.0307(11)	0.2034(2)	0.1116(1)
C(3)	0.160	0.217	0	0.1727(12)	0.2340(9)	0.000(1)
H(1)	0.133	0.020	0.272	0.1436	0.0217	0.3019
H(2)	−0.048	0.322	0.171	−0.0523	0.3471	0.1903
H(3)	0.140	0.350	−0.071	0.1511	0.3776	−0.0788
H(3′)	0.293	0.237	0.071	0.3162	0.2559	0.0789

potential parameters (Mirsky 1978). The cluster was a super-cell of the tetragonal cell with each dimension increased to seven times that of the original cell. Total energy was calculated for various values of rigid rotation about c-axis of the central molecule of the cluster. At each pressure the angle of rotation was obtained from energy minimization. In figure 7 we compare the angle of rotation corresponding to the minimum energy with the values obtained from x-ray data and find that there is good agreement between these two. Thus the assumption of a rigid molecule is valid in this low pressure region and molecular deformation starts above 12 GPa. Also this implies that the intermolecular H . . . H separation drives the molecular deformation above 12 GPa and hence will have crucial role in the subsequent phase transitions.

The variation of c/a ratio in the tetragonal phase is shown in figure 8. A scatter in the data higher than the experimental error is seen around 2.8 and 9 GPa. It is to be noted that Raman spectra also showed splitting of modes at these pressures (Rekha Rao *et al* 2000). However, from the fact that in the present ADXRD studies we can index the data using a tetragonal cell unambiguously up to 12 GPa, the occurrence of any structural phase transition

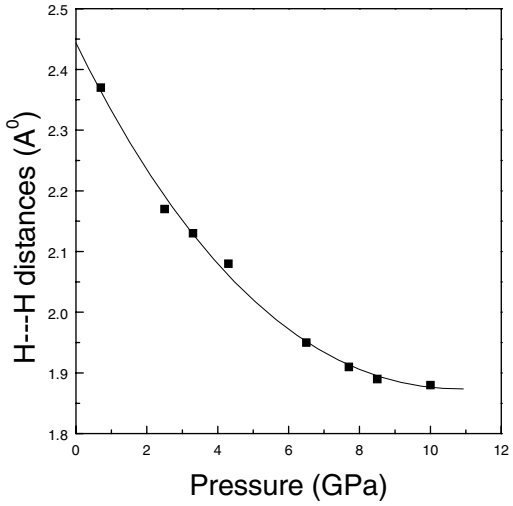

Figure 6. The variation of H . . . H separation with pressure obtained from Rietveld refinements.

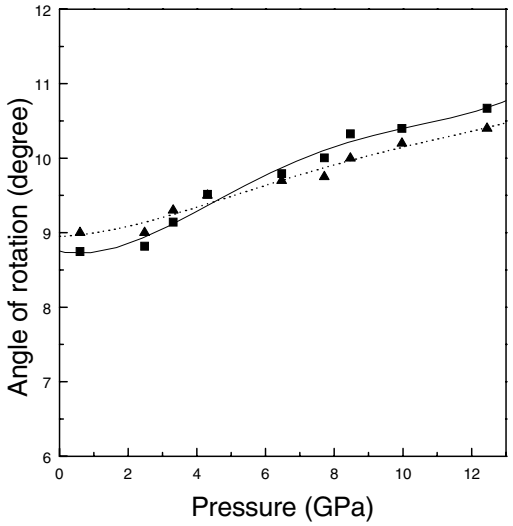

Figure 7. The variation of the intermolecular angle of rotation of the two adamantane molecules with pressure. The solid line represents the fitted data obtained from Rietveld refinements (■) and the dotted line is obtained from energy minimization (▲).

is ruled out in this pressure region. This is compatible with the fact that the number of observed Raman modes is less than those expected for tetragonal phase even after the observed mode splitting and hence these changes could be due to anisotropy in compression leading to further lifting of accidental mode degeneracy. Above 12.5 GPa, c/a decreases rapidly in the pressure region where the R factor in Rietveld refinements starts increasing rapidly. Thus based on the above analysis we conjecture that distortion of the adamantane molecule sets in around 9 GPa when H . . . H separation tends to saturate near the critical value of 1.9 Å as seen in figure 6. Thus it is reasonable to assume that with further increase of pressure, faster increase in the molecular distortion will result in structural transition to lower symmetry. This correlates with

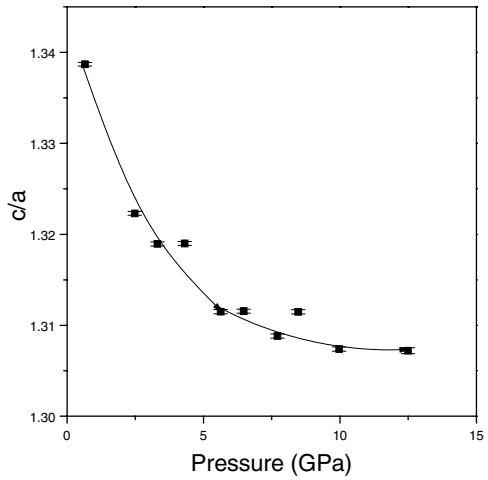

Figure 8. c/a variation with pressure in the tetragonal phase. The experimental data points along with error bars are shown. The line is only to guide the eye and to highlight the deviations close to 2.8 GPa and 9 GPa. The standard deviations in a and c are 0.0004 and 0.0007 at 0.7 GPa, 0.0005 and 0.0013 at 12.5 GPa respectively, which are well below the scatter in the data.

the changes observed in the Raman spectra and x-ray data around 16 GPa. It is interesting to note that the phase diagram of adamantane (Herbstein 1996) has a cubic–tetragonal–melt triple point close to 700 K and 2.7 GPa, implying the existence of another phase boundary that will intersect the pressure axis above 2.7 GPa. The existence of such a phase boundary is consistent with our above conclusion. This and the fact that two new lines not allowed by the space group appeared at 16 GPa supports the belief that this change is not due to pressure gradient that may have developed.

The structural change above 22 GPa can be related to the splitting of the C–C stretching modes in Raman spectra (Rekha Rao *et al* 2000) and results from the lowering of the crystal symmetry. The small discrepancy in the transition pressure is due to the continuous nature of the transition consistent with the fact that the tetragonal and monoclinic structures are closely related.

The volume per molecule at each pressure was obtained by least squares fitting of all the distinct lines to the tetragonal or monoclinic cell as the case may be. The room temperature P–V isotherm (EOS) is shown in figure 9. In this we have also included the experimental data points of Ito (1973) in the cubic phase up to the disorder–order transition and that of Vaidya and Kennedy (1971) in the tetragonal phase. The bulk modulus (B) and its pressure derivative (B') obtained by fitting the data up to 12 GPa to a universal equation of state (Vinet *et al* 1987) are 1.02 GPa and 11.1 respectively. An extrapolated zero pressure volume of 229.0 Å^3 per molecule for the tetragonal phase yields the best fit to the data. The small bulk modulus is consistent with the fact that the intermolecular bonding is weak and compression is essentially achieved by reduction of the intermolecular space. These values may be compared with that of C_{60} ($B = 18.1$ GPa and $B' = 5.7$), another globular molecular solid.

To conclude, adamantane undergoes a series of structural changes under pressure as expected. In the 0.7–5.0 GPa pressure region there is a rapid variation in the c/a ratio and close to 10.0 GPa there is a kink, which is found to be coincident with the onset of molecular distortion. The appearance of two new lines and significant change in the intensities of diffraction lines with increased background noticed above 16 GPa imply a change of structure.

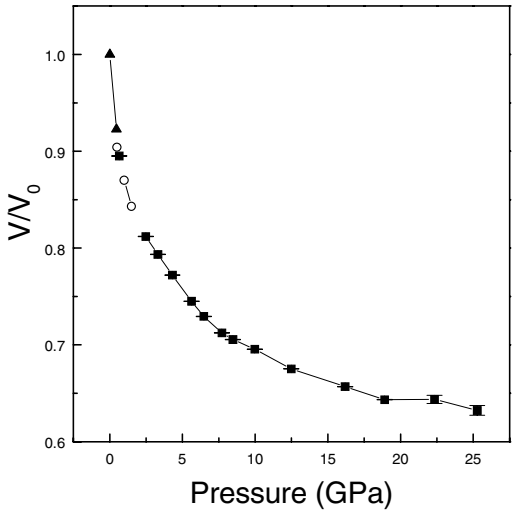

Figure 9. EOS of adamantane. The solid squares are experimental data points. Error bars on V/V_0 are also plotted. Solid triangles (▲) are from Ito (1973). The open circles show the data from Vaidya and Kennedy (1971).

The diffraction data also clearly indicate a structural phase transition above 22 GPa. The present high pressure x-ray work thus corroborates the spectral changes observed in Raman measurements. These can now be associated with subtle isostructural or structural phase changes. More data at closely spaced pressure intervals are desirable for the unambiguous confirmation of the c/a variation with pressure. Also a neutron scattering measurements under pressure is needed to confirm the crucial role played by hydrogen atoms which are central to these phase changes in adamantane.

Acknowledgment

ADXRD measurements were carried out at SPRING-8, Japan, under proposal no 1998A0272-ND-NP and with travel support from the Department of Science and Technology, Government of India. We gratefully acknowledge the help received from Dr Y Katayama, Professor O Shimomura and Professor Kawamura during the measurements at SPRING-8.

References

Amoureux J P and Foulon M 1987 *Acta Crystallogr.* B **43** 470

Chandrabhas N, Sood A K, Muttu D V S, Sunder C D, Bharathi A, Hariharan Y and Rao C N R 1994 *Phys. Rev. Lett.* **73** 3411

Gualtieri A, Norby P, Hanson J and Riljac J H 1996 *J. Appl. Crystallogr.* **29** 707

Hamilton W C 1968 *Hydrogen Bonding in Solids, Methods of Structure Determination* (New York: Brookhaven National Laboratory) p 52

Herbstein F H 1996 *J. Mol. Struct.* **374** 111

Immirzi A 1980 *Acta. Crystallogr.* B **36** 2378

Ito T 1973 *Acta. Crystallogr.* B **29** 364

Katoh E, Yamawaki H, Fujihisa H, Sakashita M and Aoki K 1999 *Phys. Rev.* B **59** 11 244

Mirsky K 1978 *Computing in Crystallography, Proc. Int. Summer School in Crystallographic Computing* (Twente: Delft University Press) p 169

Pilati T 1998 *J. Appl. Crystallogr.* **31** 503
Rekha Rao, Sakuntala T, Deb S K, Roy A P, Vijayakumar V, Godwal B K and Sikka S K 1999 *Chem. Phys. Lett.* **313** 749
——2000 *J. Chem. Phys.* **112** 6739
Sikka S K 1997a *Ind. J. Pure Appl. Phys.* **35** 677
——1997b *Curr. Sci.* **73** 195
Sikka S K and Sharma S M 1992 *Curr. Sci.* **63** 317
Shirl M, Breitline M, Jones A D and Boyd R H 1971 *J. Chem. Phys.* **54** 3959
Snoke D W, Raptis Y S and Syassen K 1992 *Phys. Rev.* B **45** 14 419
Steiner Th and Saenger 1991 *Acta Crystallogr.* B **47** 1022
Vaidya S N and Kennedy G C 1971 *J. Chem. Phys.* **55** 987
Vijayakumar V and Meenakshi S 2000 *BARC Report* in preparation
Vinet P, Smith J R, Ferrante J and Rosse J H 1987 *Phys. Rev.* B **35** 1945